^{1}H NMR Studies on Cyclo[-Arg(Mtr)-Gly-Asp(Bu^t)-Ser(Bu^t)-Lys(Boc)-] and Cyclo(-Arg-Gly-Asp-Ser-Lys-), Cyclic Analogues of the 'Adhesion' Domain of Fibronectin

Michael P. Williamson,†[a] John S. Davies*[b] and W. Anthony Thomas[a]
[a] *Roche Products Ltd., PO Box 8, Welwyn Garden City, Hertfordshire AL7 3AY, UK*
[b] *Department of Chemistry, University College of Swansea, Singleton Park, Swansea SA2 8PP, UK*

High-field ^{1}H NMR techniques in DMSO solution, augmented by a comparison with calculated conformations based on cyclo(-Ala-Gly-Ala-Ala-Ala-), and restrained molecular dynamics calculations have revealed preferred conformations for both of the conformationally constrained -Arg-Gly-Asp-Ser- analogues studied. A type II'β-turn spanning Gly-Asp and a slightly less stable γ-turn at the Lys residue were revealed for both peptides.

Cell adhesion by the glycoprotein fibronectin has been intensively studied[1] in recent years, and the focal point of its adhesion characteristics has been identified[2] as a tetrapeptide sequence, -Arg-Gly-Asp-Ser-, located in a 90-residue (11.5 kDa) domain in the middle of the protein. Variations can be tolerated in the fourth residue, serine, but the fundamental requirement appears to be an -Arg-Gly-Asp- sequence within a β-turn loop. Analogues with very conservative residue replacements failed to inhibit cell adhesion in a competitive inhibition study,[3] implying that there is a need for a strict conformational relationship between the guanidyl side-chain of arginine and the carboxyl side-chain of the aspartyl residue.

Recently it has been established[4] that the cells mediate their recognition for the -Arg-Gly-Asp- domain in fibronectin *via* the integrin family of surface proteins, which includes the fibronectin and vitronectin receptors. The integrins appear to have an influence on a number of key processes, including cell anchorage, differentiation and migration, and are involved in a critical manner in a wide range of control mechanisms, *e.g.* tumour metastasis and blood clotting. Although the receptors share an ability to recognise -Arg-Gly-Asp-, their ligand specificities vary. Thus, replacement[5] of L-Ser by D-Ser in the substrate peptide H-Gly-Arg-Gly-Asp-Ser-Pro-Cys-OH had an effect on the vitronectin but not the fibronectin interaction, while L-Asn for L-Ser increased interaction with the latter receptor. Of more spectacular significance, however, was the 10 000-fold higher affinity for the vitronectin than for the fibronectin receptor shown by the cyclic analogue[5,6] H-Gly-Pen-Gly-Arg-Gly-Asp-Ser-Pro-Cys-Ala-OH (where Pen = penicillamine).

It is this quest for a better understanding of the conformational requirements involved in cell recognition that underpins our interest in the title cyclic analogues containing the -Arg-Gly-Asp-Ser- sequence. In our choice of target molecule our aim was to make the cyclic analogue as conformationally tight as possible, while aiming to maintain a β-turn environment over the -Arg-Gly-Asp- trio of residues. The advantage of the lysine residue as the 'linker' to close the pentapeptide ring was the availability of its side-chain for immobilising the cyclic analogue on to solid matrices, which might be a better mimic for cell adhesion than the free peptide, and on to glass, which would aid the study of adhesion *via* optical microscopy. Our preliminary studies on development work in this field have already been reported[7] in brief.

† *Present address:* Krebs Institute for Biomolecular Research, Department of Molecular Biology and Biotechnology, University of Sheffield, Sheffield S10 2TN, UK.

Fmoc-Asp(Bu^t)-Ser(Bu^t)-Lys(Boc)-Arg(Mtr)-Gly-PepsynK
↓ 1% TFA–CH_2Cl_2
Fmoc-Asp(Bu^t)-Ser(Bu^t)-Lys(Boc)-Arg(Mtr)-Gly-OH
↓ Piperidine–DMF
H-Asp(Bu^t)-Ser(Bu^t)-Lys(Boc)-Arg(Mtr)-Gly-OH
↓ DPPA–KH_2PO_4[9] or EDC–DMAP[10]
Cyclo[-Arg(Mtr)-Gly-Asp(Bu^t)-Ser(Bu^t)-Lys(Boc)-] **1**
↓ 95% TFA
Cyclo[-Arg-Gly-Asp-Ser-Lys-] **2**

Scheme 1

The synthesis and biological properties of the cyclic analogues are the subject of another publication.[8] The outline synthetic route is summarised in Scheme 1. The cyclopeptide **2** was obtained as its trifluoroacetate salt, but for biological testing it had to be converted into its acetate analogue because of the sensitivity of the test cells to trifluoroacetate. This paper reports detailed NMR studies at high field on the cyclopeptide analogues **1** and **2**.

Results and Discussion

Measurement of NMR Parameters for cyclo[-Arg(Mtr)-Gly-Asp(Bu^t)-Ser(Bu^t)-Lys(Boc)-] **1** *and* cyclo[-Arg-Gly-Asp-Ser-Lys-] **2**.—*Assignment of NMR spectrum.* Most studies were carried out in deuteriated dimethyl sulphoxide ([$^2H_6$]DMSO) solutions using 2–5 mg of peptide per 0.5 cm^3. The 1D spectrum of the deprotected peptide **2** at 500 MHz is shown in Fig. 1. Spin systems for both peptides were assigned independently by the use of COSY and TOCSY 2D spectra (not shown). The spectra are simple enough that assignments can be made by inspection, relying on the difference between the chemical shifts of C$^\beta$H protons for Ser and Asp residues to distinguish these two residues. Arg and Lys were distinguished by observing relays to the side-chain amide proton of Arg, and all assignments were confirmed by sequential NOEs. Chemical shift assignments are given in Table 1.

Measurement of conformational parameters. The three-bond coupling constants $^3J_{HN\alpha}$ were obtained from well-digitised 1D spectra. The temperature coefficients of the amide protons were determined by least-squares fitting to spectra acquired at 26, 31, 36 and 41 °C. For the deprotected peptide **2**, a further indication of amide proton hydrogen bonding was obtained by

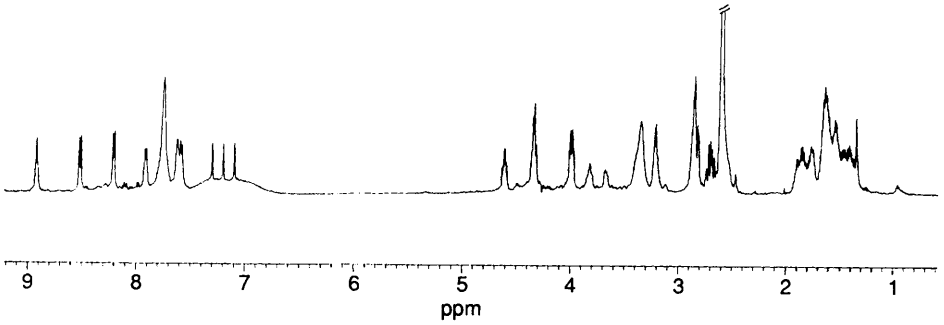

Fig. 1 500 MHz 1D spectrum of cyclo(-Arg-Gly-Asp-Ser-Lys-) **2** in DMSO at 27 °C. The three signals centred around 7.19 ppm come from ammonium ions.

Table 1 Chemical shift assignments for protected and deprotected peptide[a]

	NH	α	β	Other
Protected[b]				
Arg	8.02	4.27	1.77, 1.58	γ ~1.5, δ 3.15, NHε ~6.5
Gly	8.95	3.99, 3.41		
Asp	8.43	4.60	2.78, 2.64	
Ser	7.55	4.29	3.65, 3.53	
Lys	8.18	3.87	1.93, 1.79	γ,δ 1.4, ε 2.97, NHε 6.83
Deprotected				
Arg	7.91	4.32	1.77, 1.60	γ ~1.63, δ 3.30
Gly	8.92	3.99, 3.47		
Asp	8.53	4.61	2.80, 2.69	
Ser	7.59	4.33	3.81, 3.66	
Lys	8.21	3.97	1.96, 1.85	γ,δ ~1.55, ε 2.84

[a] Shifts relative to DMSO = 2.6 ppm from TMS. [$^2H_6$]DMSO solution at 26 °C. [b] Protecting group signals were observed at 1.45, 1.50 (OBu^t), 1.25 (Boc Bu^t), 2.15, 2.6 and 2.70 (ArMe), 3.90 (ArOMe) and 6.77 (ArH).

Table 2 Conformation-dependent NMR parameters

	Arg	Gly	Asp	Ser	Lys
Protected					
$^3J_{HN\alpha}$[a]	8.1	11.6[b]	8.3	8.0	7.0
δ/T[c]	−3.8	−6.1	−8.0	−1.2	−7.7
Deprotected					
$^3J_{HN\alpha}$[a]	8.3	11.3[b]	8.1	8.3	7.1
δ/T[c]	−1.3	−5.4	−7.0	−0.8	−3.2
$CDCl_3$[d]	−1.6	−6.1	−18.7	5.1	−3.7

[a] Three-bond coupling constant between HN and C$^\alpha$H in Hz. [b] Sum of both values. [c] Temperature dependence of NH shift, in ppb/K (ppm × 10^{-3}/K). A negative sign indicates an upfield shift with increase in temperature. [d] Shift in Hz on adding $CDCl_3$ to a DMSO solution (1:5 v/v). Upfield shifts are negative.

stepwise addition of $CDCl_3$ to the DMSO solution. The results of these experiments are given in Table 2.

Further conformational information came from the nuclear Overhauser effect. For the protected peptide **1**, the correlation time of the molecule was such that it gave good NOESY cross-peaks. A NOESY spectrum acquired with a mixing time of 200 ms was used for the initial assignment of cross-peaks and for confirmation of the spin system assignments by sequential assignment, but to avoid possible spin diffusion effects, a mixing time of 100 ms was used subsequently to provide more reliable cross-peak intensities. Interatomic distances were then obtained from the cross-peak intensities by assuming a direct r^{-6} relationship between interatomic distance and cross-peak intensity.

The deprotected peptide **2** has a somewhat shorter correlation time in DMSO, such that it gave very poor NOESY spectra, necessitating the use of ROESY for this peptide. The ROESY spectrum is shown in Fig. 2 with positive and negative contour levels plotted separately, for clarity. In phase-sensitive ROESY spectra, TOCSY-type coherence transfer peaks can be distinguished from true rotating frame NOEs (ROEs) by their phase: if the diagonal is plotted positive, the TOCSY-type peaks are positive, while ROE peaks are negative.[11] As can be seen from Fig. 2, there are many TOCSY-type peaks in the aliphatic region, which is useful for confirming side-chain assignments but means that cross-peak intensities in this region cannot be used for obtaining distance constraints. On the other hand, there are no TOCSY-type peaks between amide and aliphatic protons, which means that cross-peak intensities from amide protons can be used for obtaining distance constraints. This was confirmed by changing the position of the spin-locking field, which should affect the intensity of TOCSY-type peaks without affecting the intensity of ROE peaks. TOCSY transfer is most efficient between pairs of resonances that are positioned either side of the spin-locking field frequency at the same separation from it. In Fig. 2, the spin-locking field was positioned on the water resonance (3.27 ppm), which explains the distribution of TOCSY-type peaks. NOE/ROE-derived distance constraints are given in Table 3.

Structural Conclusions.—In general, an amide temperature dependence of <3 ppb K^{-1} is indicative of hydrogen bond formation.[12] A further indicator of hydrogen bonding is provided by observation of small amide shift changes on addition of chloroform.[13] The temperature and solvent dependence parameters given in Table 2 clearly indicate that the

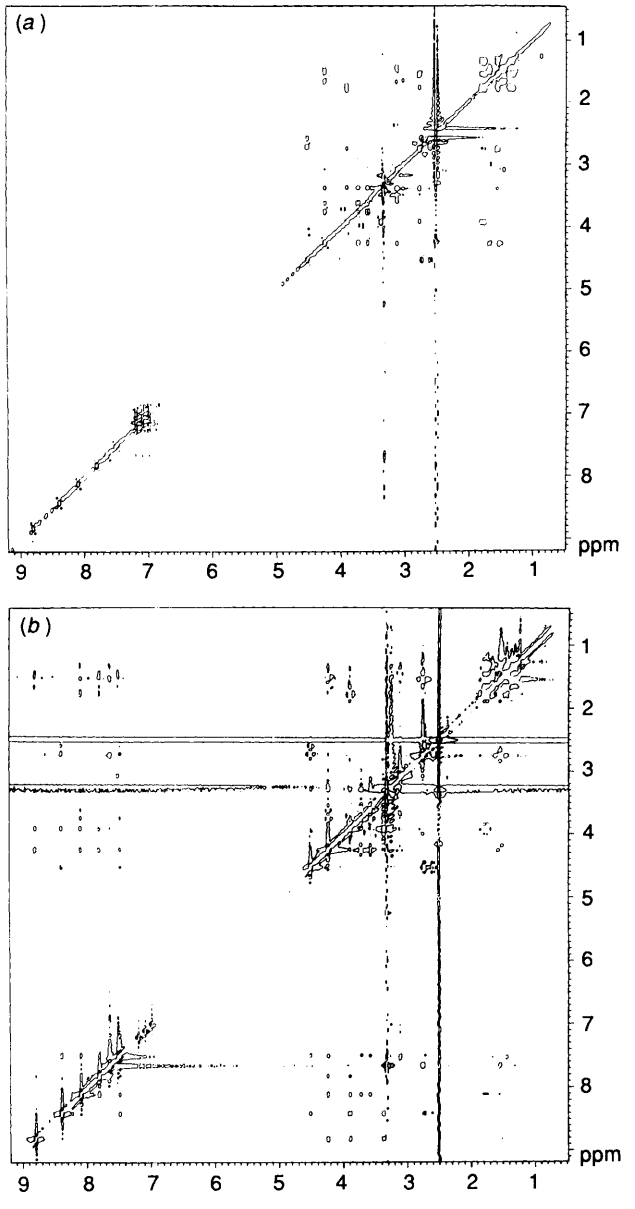

Fig. 2 500 MHz ROESY spectrum of deprotected peptide in DMSO at 27 °C: (*a*) positive contour levels (TOCSY-type peaks); (*b*) negative contour levels (rotating frame NOE peaks)

amide proton of Ser is hydrogen bonded in both protected and deprotected peptides, and that the amide proton of Arg is hydrogen bonded in the deprotected peptide **2** but only partially hydrogen bonded in the protected peptide **1**. The only possible hydrogen bonding arrangement for the Arg proton is a γ-turn to the carbonyl group of Ser (Fig. 3), but there are two possible hydrogen bonding arrangements for the Ser NH: a β-turn to the Arg carbonyl [Fig. 3(*a*)] or a γ-turn to the Gly carbonyl [Fig. 3(*b*)].[14,15] Cyclic peptides studied to date prefer β-turns. For example, Kessler has studied a number of thymopoietin analogues,[15] all of which have β-turns. The values marked * in Table 3 are typical of NOEs observed in Kessler's thymopoietin analogues, implying the presence of a β-turn in our cyclic peptides also. The further observation of the NOEs marked † in Table 3 is a strong indication that the Arg, Lys and Ser NHs are all on the same side, and that one of the most likely conformations achieved by the peptides is the one shown for peptide **1** in Fig. 4.

Comparison with calculated conformations. Despite the strength of the above arguments, a more objective assessment of the conformation would be desirable. NMR studies of peptide conformation have always been bedevilled by subjective decisions, both because of the flexibility of peptides in solution and because of the difficulty of considering all possible conformations that may be consistent with the data. We have therefore tried to introduce more objectivity into the structural analysis by generating a database (containing 47 structures) that contains all the backbone conformations that are energetically likely, and then systematically comparing each conformation in the database with the NMR data in order to characterise those conformations that are consistent with the data. In this way we can build up a comprehensive and unbiased list of all possible conformations that are consistent with the NMR data.

Table 3 Distance constraints derived from NOE and ROE data[a]

Protected
R_N to R_α 2.86, K_N 2.63,† K_α 3.17
G_N to G_α 3.18/3.36, R_N 4.03, R_α 2.65*
D_N to D_α 3.16, G_N 3.61, G_α 2.53*/long
S_N to S_α 3.06, D_N 2.80,* D_α 3.42
K_N to K_α 2.65, S_N 3.37,† S_α 2.91,† S_β 3.31
Deprotected
R_N to R_α 2.94, K_N 2.50,† K_α 3.17
G_N to G_α 2.79/2.73, R_α 2.61*
D_N to D_α 3.04, G_α 2.73/2.65*
S_N to S_α 2.88, D_N 2.70,* D_α 2.99
K_N to K_α 2.78, S_N 2.93, S_α 2.83,† S_β 3.00/3.14

[a] All distances in Å; entries marked *·† are discussed in the text. R, G, D, S, K refer to Arg, Gly, Asp, Ser, Lys, respectively.

Initial trials demonstrated the importance of including the hydrogen bonds in the fitting of the measured NMR parameters to the calculated conformations, and we therefore fitted the 47 calculated conformations to four different NMR-derived distance constraint sets, differing in the hydrogen bond distances that were required to be satisfied: (*a*) NOEs only; (*b*) NOEs plus the Ser NH–Arg CO H-bond; (*c*) NOEs plus the Ser NH–Gly CO H-bond; and (*d*) NOEs plus Ser NH–Arg CO and Arg NH–Ser CO H-bonds.

A summary of the results for peptide **2** is given in Table 4. Similar results were obtained for the protected peptide **1**. Table 4 also contains the results from fitting the calculated conformations to the observed $^3J_{HN\alpha}$ coupling constants.

The only structures that fit the γ-turn Ser NH–Gly CO H-bond constraint [Fig. 3(*b*); case (c) in Table 4] have a large separation between Asp NH and Ser NH (*i.e.* the Asp NH is forced to point out of the ring), which conflicts with the strong NOE seen between these two protons. Kessler has also noted the characteristic short distance between these two amide protons in type II′ β-turns.[15] This provides strong confirmation of our previous conclusion that the data are only consistent with the β-turn hydrogen bond between Ser NH and Arg CO, as shown in Fig. 3(*a*). *J*-coupling data also militate against a Ser NH–Gly CO H-bond.

Conformational details. From Table 4, the three structures 1, 7 and 8 emerge as conformations that fit the NMR data roughly equally well. Structure 9 is also reasonably well fitted, except for an unacceptably large violation of the Ser NH–Arg CO hydrogen bond constraint, which makes it an unlikely structure. Structure 9 is therefore not considered further. Structure 1 is calculated to be 0.8 kcal mol^{-1} ‡ more stable than structures 7 and 8; the Boltzmann distribution predicts relative populations for structures 1, 7 and 8 of 67:17:16, respectively, at room

‡ 1 cal = 4.184 J.

Table 4 Comparison of NOE distance constraints to model structures for deprotected peptide[a]

		NOE constraints						H-bond constraints			RMS total violation[b]				
Atom pair:		R_N–K_N	G_N–R_α	S_N–D_N	S_N–D_α	K_N–S_N	K_N–S_α	S_N–R_{CO}	R_N–S_{CO}	R_N–G_{CO}	(a)	(b)	(c)	(d)	
Distance:		2.50	2.61	2.70	2.99	2.93	2.83	2.50	2.50	2.50					
Structure no.	E[c]														Violation of $^3J_{HN\alpha}$
1	6.98	0	0	0	6	0	8	13	22	25	12	18	26	27	3.0
2	7.14	0	0	0	6	0	8	22	23	25	12	25	26	33	3.6
3	7.27	0	0	0	6	0	8	23	25	24	12	26	25	35	3.8
4	7.38	0	10	0	6	0	8	35	22	23	15	38	26	43	4.6
5	7.64	0	0	16	0	9	8	35	24	12	21	41	23	46	5.0
6	7.74	0	0	14	0	8	8	32	23	3	19	37	19	43	4.7
7	7.80	12	0	0	6	11	0	13	0	28	18	22	32	22	2.4
8	7.80	13	0	0	6	12	0	12	0	27	19	23	32	23	2.4
9	7.84	13	0	0	6	10	0	21	0	27	18	28	31	28	2.9
10	8.19	13	10	0	6	14	0	37	0	23	23	43	31	43	4.5
11	8.28	0	10	10	6	0	8	26	24	0	18	32	18	39	4.2
12	8.34	12	10	0	6	11	0	39	0	25	21	44	31	44	4.6

[a] Some of the distance constraints listed in Table 2 are not included here, as the violations are small and not highly structure dependent; however, they were used for the calculation of the RMS violations of distance constraints. Constraints to $G^\alpha H$ protons were not used because of a lack of stereospecific assignments. All distance violations are given in 10^{-1} Å. Residues are labelled R, G, D, S, K for Arg, Gly, Asp, Ser, Lys, respectively. Only the first 12 structures are listed. [b] The RMS violation is listed for the four cases described in the text. When different values were used for the calibration from NOE intensity to distance, the sizes of the violations of NOE constraints altered, but the rank ordering of structures did not. [c] Calculated conformational energy, in kcal mol^{-1}.

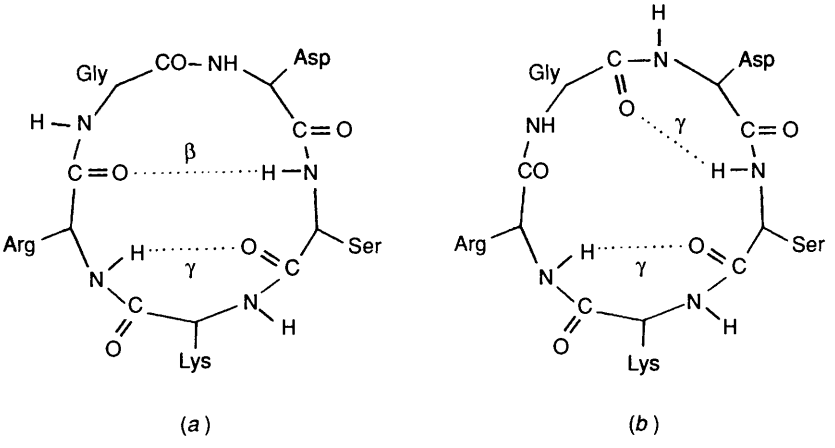

Fig. 3 Schematic diagram of the two possible backbone hydrogen bonding arrangements, with Ser NH and Arg NH both hydrogen bonded: (*a*) β-turn/γ-turn; (*b*) γ-turn/γ-turn

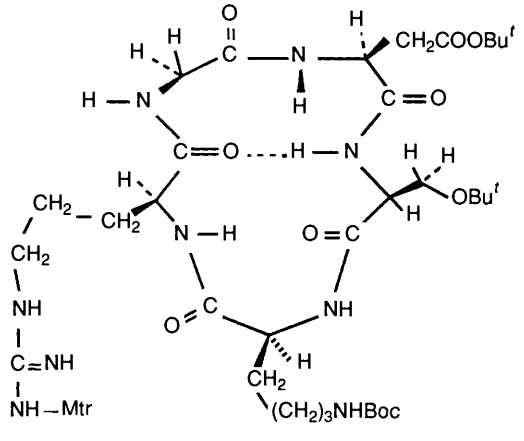

Fig. 4 Most likely peptide backbone conformation of cyclopeptide **1** in DMSO solution

temperature. The backbone dihedral angles for these three conformations are given in Table 5. All three have a β-turn centred on residues Gly and Asp. In structures 7 and 8, which are very similar, this is a type II′ turn, while in structure 1 it is a type V′ turn, described by Richardson[16] as a distorted II′ turn. Some sort of type II′ turn might be expected, since a number of cyclic pentapeptides have been observed to prefer a type II′ structure at Gly–X or D-residue–X sequences.[15,17] The γ-turn at Lys is only present in structures 7 and 8.

To demonstrate that there are low-energy structures that fit the NMR data and that resemble structure 1, but contain both a β-turn and a γ-turn, we took structure 1 and subjected it to a restrained molecular dynamics calculation at 300 K. The resulting structure, shown in Fig. 5, is of low energy and fits the NOE constraints with a root-mean-square deviation of 0.11 Å, with the largest single constraint violation being 0.23 Å (for the Lys NH–Ser $C^\alpha H$ constraint). It contains a type II′ β-turn and a γ-turn, with well-formed hydrogen bonds across both turns. No effort was made to alter the side-chains back to the true functionality, because NMR data indicate very little preferred conformation for the side-chains.

The question that now arises is whether the actual solution conformation is rigid and like that shown in Fig. 5, or whether it is in rapid equilibrium between a set of conformations similar in nature both to Fig. 5 and to structures 1, 7 and 8. The NMR data suggest that the structure of the peptide in solution is not

Table 5 Backbone dihedral angles/° for structures 1, 7 and 8

Structure	ϕ_{Arg}	φ_{Arg}	ϕ_{Gly}	φ_{Gly}	ϕ_{Asp}	φ_{Asp}	ϕ_{Ser}	φ_{Ser}	ϕ_{Lys}	φ_{Lys}
1	−115	103	90	−66	−91	63	−108	−62	102	−53
7	−105	103	91	−72	−115	−69	−92	85	80	−60
8	−113	106	90	−72	−111	−64	−108	97	79	−61

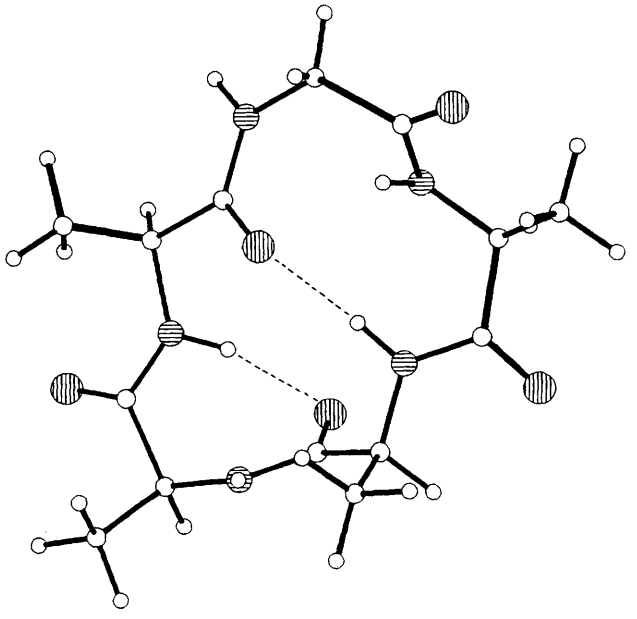

Fig. 5 Ball-and-stick model of a low-energy structure derived from structure 1 by restrained molecular dynamics. The structure was constrained to contain the hydrogen bonds Ser NH–Arg CO and Arg NH–Ser CO.

completely rigid. This is indicated by the 'averaged' values of the coupling constants, and by the loss in differentiation in NMR parameters on comparing the deprotected with the protected peptide, suggesting a loss in conformational rigidity in the protected peptide. Furthermore, amide temperature coefficients measured for the rigid cyclic peptide thymopoietin showed more extreme values than seen here (for example, zero or even slightly positive values for the γ-turn residue equivalent to the Lys residue), again implying a lack of rigidity in peptides **1** and **2**. The small energy differences between many of the calculated structures would also imply the likelihood of conformational mobility. The most reasonable interpretation of the NMR data is therefore that the peptide is equilibrating rapidly between several conformations, among which structures similar to 1, 7 and 8 predominate.

The idea of a set of equilibrating conformations is supported by comparison of the NOE violations in the three structures. The largest violations in structure 1 are satisfied in structures 7 and 8 (e.g. Lys NH to Ser C$^{\alpha}$H and Arg NH to Ser CO) and, conversely, the largest violations in structures 7 and 8 are satisfied in structure 1 (*e.g.* Lys NH to Ser NH and Lys NH to Arg NH). An r^{-6} time average of the relevant distances, which would reflect the true NOE expected in equilibrating systems,[18] would therefore give much better agreement to the NOE data than any single structure on its own; in other words, good agreement with the observed NOEs would be obtained by rapid equilibration between structures 1, 7 and 8.

In this work, we have not considered the possibility of hydrogen bonding to side-chains. However, the observation that the fully protected peptide adopts a similar, albeit more flexible, conformation in solution to the deprotected peptide suggests that hydrogen bonds to side-chains cannot play a major part in the conformational equilibria present.

In conclusion, preferred conformations exist, and the general features of these preferred conformations are those illustrated by the structure in Fig. 5, *i.e.* a β-turn of the II′ type at Gly-Asp and a slightly less stable γ-turn at Lys. The deprotected peptide **2** is more structured in DMSO solution than the protected peptide **1**. Previous results on linear peptides based on the -Arg-Gly-Asp-Ser- sequence[19–21] have demonstrated the existence of two nested β-turns, centred on -Arg-Gly- and -Gly-Asp-, from which it is not clear whether the activity of the peptides is derived from the -Arg-Gly- turn or the -Gly-Asp- turn, or both. The cyclic peptide described here will allow us to separate the effect of the two nested β-turns by providing an example of a peptide in which only the -Gly-Asp- turn is present.

Experimental

Synthesis.—Protected cyclopeptide **1** (Scheme 1) was purified by repeated HPLC on a 25 cm × 0.4 cm C_{18} reverse phase column using MeCN–0.1% TFA (70:30 v/v). Appropriate fractions (t_R = 4.6 min, flow rate 1 cm^3 min^{-1}) were evaporated to dryness and triturated with ether to give cyclo[-Arg(Mtr)-Gly-Asp(Bu^t)-Ser(Bu^t)-Lys(Boc)-] **1** as a white powder. (Found: C, 54.9; H, 7.2; N, 13.3. $C_{44}H_{73}N_9O_{13}S$ requires C, 54.6; H, 7.4; N, 13.02%.) FAB-MS gave a strong peak at *m/z* 968 ($M^+ + 1$).

Cyclopeptide **1** in trifluoroacetic acid was left to stand overnight at room temperature, and the resultant deprotected cyclopeptide **2** was purified by removal of acid, trituration with ether and very extensive recycling through a 30 cm × 0.2 cm C_{18} Bondapak column using MeCN–0.1% TFA (70:30 v/v) as eluent. Fractions t_R = 2.87 min (flow rate 1 cm^3 min^{-1}) were combined, solvent was evaporated and the buff-coloured solid triturated with ether. The solid was used for NMR and had a strong FAB-MS ($M^+ + 1$) ion at *m/z* 544.

NMR Experiments.—Experiments were carried out on solutions (0.5 cm^3) of the peptide (2–5 mg) in [$^2H_6$]DMSO or mixtures of [$^2H_6$]DMSO with $CDCl_3$. No concentration dependence of NMR parameters was observed in DMSO. Experiments were carried out on a Bruker AM-400 spectrometer, except for the ROESY experiments on the deprotected peptide **2**, which were carried out on a Bruker AM-500.

1D NMR spectra were acquired into 32K data points and Fourier transformed with zero filling into 64K points for accurate measurement of coupling constants. 2D spectra were acquired into 256–300 files of 1K data points, and Fourier transformed using zero filling up to 2K × 2K points, using a shifted sine bell window. All 2D spectra were acquired using TPPI in the phase-sensitive mode. COSY spectra were acquired as double-quantum filtered COSY spectra, using a novel phase cycle to avoid rapid pulsing artefacts.[22] TOCSY spectra were acquired using a *z*-filter,[23] with spin locking provided by a WALTZ-16 pulse sequence. NOESY spectra were acquired at 25 °C using a mixing time of 100 ms, randomly altered by 5%. ROESY spectra were acquired at 27 °C using a mixing time of 100 ms. Spin locking was achieved by a continuous 17 kHz field, which was also used for the 90° pulses. The intensity of NOESY

and ROESY cross-peaks was measured by integrating the cross-peak volumes, using Bruker software. Where possible, intensities were taken as the mean of the values obtained for the symmetry-related cross-peaks on either side of the diagonal. Cross-peak intensities were converted into distance constraints by calibrating on sequential d_{NN} and $d_{\alpha N}$ cross-peak intensities.

Calculations.—Conformational searches were performed using the program MOLOC.[24] A cyclic peptide, cyclo(-Ala-Gly-Ala-Ala-Ala-), was constructed, and possible conformations were generated by systematic application of spherical harmonic functions. A total of 1257 conformations were generated, but after energy minimisation this number reduced to 49, with energies ranging from 6.9–16.1 kcal mol^{-1}. Each of these conformations was then compared with the distance constraints calculated from NOESY or ROESY spectra and to constraints from spin–spin couplings, to obtain a root-mean-square measure of its goodness of fit.

Restrained molecular dynamics calculations were carried out using the program CHARMM (version 19), as described.[25] Structure 1 was energy miminised, heated to 300 K, and equilibrated at 300 K for a total of 13 ps with gradually increasing weighting of distance constraints, to a maximum energy penalty of

$$E = 2(kT/2)[(r - r_0)/\delta r]^2$$

The structure was then quenched over 4.5 ps to near 0 K and energy minimised.

Acknowledgements

We are indebted to Dr. Gareth Jones, King's College London, for alerting us to the significance of the molecules; to Drs. Paul Gerber, Toni Kröhn and Neera Borkakoti for help with the computing and graphics; Dr. Lu-Yun Luan, Leicester for assistance with the 500 MHz spectra; and the SERC for financial support.

References

1 E. Ruoslahti, *Annu. Rev. Biochem.*, 1988, **57**, 375.
2 M. D. Pierschbacher and E. Ruoslahti, *Nature (London)*, 1984, **309**, 30; E. Ruoslahti and M. D. Pierschbacher, *Cell*, 1986, **44**, 517.
3 M. Ginsberg, M. D. Pierschbacher, E. Ruoslahti, G. Marguerie and E. Plow, *J. Biol. Chem.*, 1985, **260**, 3931.
4 E. Ruoslahti and M. D. Pierschbacher, *Science*, 1987, **238**, 491.
5 M. D. Pierschbacher and E. Ruoslahti, *J. Biol. Chem.*, 1987, **262**, 17 294.
6 T. Siahann, L. R. Lark, M. D. Pierschbacher, E. Ruoslahti and L. M. Gierasch, in *Peptides: Chemistry, Structure and Biology*, ed. J. E. Rivier and G. R. Marshall, Escom, Leiden, 1990, p. 699.
7 J. S. Davies, G. E. Jones and J. J. A. Orchison, in *Peptides 1988*, ed. G. Jung and E. Bayer, W. de Gruyter, Berlin, 1989, p. 408; G. E. Jones, R. G. Arumugham and M. L. Tanzer, *J. Cell. Biol.*, 1986, **103**, 1663.
8 J. S. Davies, G. E. Jones and J. J. Orchison, in preparation.
9 S. F. Brady, W. J. Palevada, B. H. Arison, R. M. Friedlinger, R. F. Nutt and D. F. Veber, in *Proceedings of the 8th American Peptide Symposium*, ed. V. J. Hruby and D. H. Rich, Pierce Chemical Co., Rockford, Illinois, USA, 1983, p. 127.
10 H. Kessler and B. Kutscher, *Liebigs Ann. Chem.*, 1986, 869.
11 D. Neuhaus and M. P. Williamson, *The Nuclear Overhauser Effect in Structural and Conformational Analysis*, VCH Publishers, New York, 1989, p. 326.
12 H. J. Dyson, M. Rance, R. A. Houghten, R. A. Lerner and P. E. Wright, *J. Mol. Biol.*, 1988, **201**, 161.
13 D. W. Urry and M. M. Long, *CRC Crit. Rev. Biochem.*, 1976, **4**, 1.
14 H. Kessler, *Angew. Chem., Int. Ed. Engl.*, 1982, **21**, 512.
15 H. Kessler, B. Kutscher and A. Klein, *Liebigs Ann. Chem.*, 1986, 893.
16 J. S. Richardson, *Adv. Protein Chem.*, 1981, **34**, 167.
17 J. A. Smith and L. G. Pease, *CRC Crit. Rev. Biochem.*, 1980, **8**, 315.
18 A. E. Torda, R. M. Scheek and W. F. van Gunsteren, *J. Mol. Biol.*, 1990, **214**, 223.
19 J. Reed, W. Hull, W. Leith, D. Kübler, S. Suhai and V. Kinzel, *Eur. J. Biochem.*, 1988, **178**, 141.
20 W. Hull, J. Reed, W. Lieth, B. Lüning and V. Kinzel, *Computer Assisted Molecular Modelling—Applications in Molecular Biology and Perspectives for Cancer Research*, Deutsches Krebsforschungszentrum, Heidelberg, Germany, 1989.
21 H. Mickos, J. Bahr and B. Lüning, *Acta Chem. Scand.*, 1990, **44**, 161.
22 A. E. Derome and M. P. Williamson, *J. Magn. Reson.*, 1990, **88**, 177.
23 M. Rance, *J. Magn. Reson.*, 1987, **74**, 557.
24 K. Müller, H. J. Amman, D. M. Doran, P. Gerber, K. Gubernator and G. Schrepfer, *Bull. Chem. Soc. Belg.*, 1988, **97**, 655; P. Gerber, K. Gubernator and K. Müller, *Helv. Chim. Acta*, 1988, **71**, 1429.
25 M. P. Williamson and V. S. Madison, *Biochemistry*, 1990, **29**, 2895.

Paper 0/04353B
Received 26th *September* 1990
Accepted 1st *November* 1990